

Detect-and-Avoid: Flight Test 6 Scripted Encounters Data Analysis

Wei-Ching Wang

*Research Engineer, Bay Systems Consulting Inc, NASA Ames Research
Center, Moffett Field, California, 94035-1000*

M. Gilbert Wu

*Research Engineer, NASA Ames Research Center, Moffett Field, California,
94035-1000*

NASA STI Program . . . in Profile

Since its founding, NASA has been dedicated to the advancement of aeronautics and space science. The NASA scientific and technical information (STI) program plays a key part in helping NASA maintain this important role.

The NASA STI Program operates under the auspices of the Agency Chief Information Officer. It collects, organizes, provides for archiving, and disseminates NASA's STI. The NASA STI Program provides access to the NASA Aeronautics and Space Database and its public interface, the NASA Technical Report Server, thus providing one of the largest collection of aeronautical and space science STI in the world. Results are published in both non-NASA channels and by NASA in the NASA STI Report Series, which includes the following report types:

- **TECHNICAL PUBLICATION.** Reports of completed research or a major significant phase of research that present the results of NASA programs and include extensive data or theoretical analysis. Includes compilations of significant scientific and technical data and information deemed to be of continuing reference value. NASA counterpart of peer-reviewed formal professional papers, but having less stringent limitations on manuscript length and extent of graphic presentations.
- **TECHNICAL MEMORANDUM.** Scientific and technical findings that are preliminary or of specialized interest, e.g., quick release reports, working papers, and bibliographies that contain minimal annotation. Does not contain extensive analysis.
- **CONTRACTOR REPORT.** Scientific and technical findings by NASA-sponsored contractors and grantees.

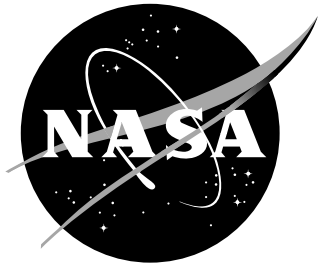
- **CONFERENCE PUBLICATION.** Collected papers from scientific and technical conferences, symposia, seminars, or other meetings sponsored or co-sponsored by NASA.
- **SPECIAL PUBLICATION.** Scientific, technical, or historical information from NASA programs, projects, and missions, often concerned with subjects having substantial public interest.
- **TECHNICAL TRANSLATION.** English-language translations of foreign scientific and technical material pertinent to NASA's mission.

Specialized services also include creating custom thesauri, building customized databases, and organizing and publishing research results.

For more information about the NASA STI Program, see the following:

- Access the NASA STI program home page at ***<http://www.sti.nasa.gov>***
- E-mail your question via the Internet to **help@sti.nasa.gov**
- Fax your question to the NASA STI Help Desk at 443-757-5803
- Phone the NASA STI Help Desk at 443-757-5802
- Write to:
NASA STI Help Desk
NASA Center for AeroSpace Information
7115 Standard Drive
Hanover, MD 21076-1320

NASA/TM-2020-220515



Detect-and-Avoid: Flight Test 6 Scripted Encounters Data Analysis

Wei-Ching Wang

*Research Engineer, Bay Systems Consulting Inc, NASA Ames Research
Center, Moffett Field, California, 94035-1000*

M. Gilbert Wu

*Research Engineer, NASA Ames Research Center, Moffett Field, California,
94035-1000*

National Aeronautics and
Space Administration

Ames Research Center
Moffett Field, California, 94035-1000

February 2020

The use of trademarks or names of manufacturers in this report is for accurate reporting and does not constitute an official endorsement, either expressed or implied, of such products or manufacturers by the National Aeronautics and Space Administration.

Available from:

NASA Center for AeroSpace Information
7115 Standard Drive
Hanover, MD 21076-1320
443-757-5802

Abstract

The Unmanned Aircraft System (UAS) in the National Airspace System (NAS) project conducted Flight Test 6 (FT6) in 2019. The ultimate goal of this flight test was to produce data to inform RTCA SC-228’s Phase II Minimum Operational Performance Standards (MOPS) for Detect and Avoid (DAA) and Low Size, Weight, and Power Sensors. This report documents the analysis of scripted encounters’ data. Scripted encounters flown were analyzed and categorized based on the outcome of alert, maneuver guidance, and effectiveness of pilots’ maneuver in resolving conflicts. Results indicate that UAS pilots’ decisions as well as intruder maneuvers are leading factors that contribute to ineffective DAA maneuvers. Results also show that adding buffers to the DAA’s suggested minimum turn angle improves effectiveness of the DAA maneuvers.

Contents

1	Introduction	4
2	Detect and Avoid	5
3	Flight Test Operations	6
3.1	Test Aircraft	6
3.2	Encounter Scenario Design	8
3.2.1	Encounter Geometry	8
3.3	Detect-and-Avoid Algorithm	11
3.4	Ground Control Station	11
3.5	Pilot’s Background & Procedure	12
3.6	Data Collection and Post-Processing	12
4	Analysis and Results	13
4.1	Flight Cards Summary	13
4.2	Categorization by Maneuver Outcomes	14
4.2.1	Flight Card Categorization Scheme & Statistics	14
4.2.2	Explanations of Categories with Examples	16
4.3	Breakdown by Surveillance Range	20
4.4	Trajectory Error Analysis	21
4.5	Buffered Heading and Encounter Effectiveness Analysis	22
5	Conclusions	23

Nomenclature

ADS-B	=	Automatic Dependent Surveillance-Broadcast
ATC	=	Air Traffic Control
CPA	=	Closest Point of Approach
DAA	=	Detect and Avoid
DAIDALUS	=	Detect and AvoID Alerting Logic for Unmanned Systems
DWC	=	DAA Well Clear
FAA	=	Federal Aviation Administration
FT6	=	Flight Test 6
GCS	=	Ground Control Station
HITL	=	Human-in-the-Loop
IP	=	Initial Point
JADEM	=	Java Architecture for DAA Extendibility and Modeling
LoDWC	=	Loss of DWC
LVC	=	Live Virtual Constructive
MOPS	=	Minimum Operational Performance Standards
NAS	=	National Airspace System
NASA	=	National Aeronautics and Space Administration
NMAC	=	Near Mid-Air Collision
RGCS	=	Research Ground Control Station
SCO	=	System Checkout
SPUT	=	Subject Pilots Under Test
SWaP	=	Low Size, Weight, and Power
Δt_{act}	=	Actual Turn Time
θ_c	=	Target Course
θ_h	=	Target Heading
Δt_{pred}	=	Predicted Turn Time
UA	=	Unmanned Aircraft
UAP	=	Unmanned Aircraft Processor
UAS	=	Unmanned Aircraft System
V_g	=	Ground Speed
\vec{V}_g	=	Ground Speed Vector
$\vec{V}_{start, M, OS}$	=	Intruder Velocity at the Start of Ownship Maneuver
$\Delta \vec{V}_{int}$	=	Change of Intruder Speed
V_{tas}	=	True Airspeed
\vec{V}_{tas}	=	True Airspeed Vector
$\vec{V}(t)_{int}$	=	Intruder Velocity
VSCS	=	Vigilant Spirit Control Station
V_w	=	Wind Speed
\vec{V}_w	=	Wind Speed Vector
WCR	=	Well Clear Recovery
\vec{w}_i	=	Initial Wind Velocity
\vec{w}_f	=	Final Wind Velocity

1 Introduction

Successful integration of Unmanned Aircraft System (UAS) operations into airspaces populated with manned aircraft relies on an effective Detect and Avoid (DAA) System. A DAA system provides surveillance, alerts, and maneuver guidance (referred to as guidance in this report) to keep a UAS “well clear” of other aircraft [1–4]. With research contributions from National Aeronautics and Space Administration (NASA), industry, and the Federal Aviation Administration (FAA), the RTCA Special Committee 228 (SC-228) published the Minimum Operational Performance Standards (MOPS) for DAA systems [5] and air-to-air radar [6] in 2017. The corresponding Technical Standard Orders (TSO), TSO-C211 and TSO-C212, were published by the FAA in October 2017. A DAA system, according to the published DAA MOPS, includes surveillance components of Automatic Dependent Surveillance-Broadcast (ADS-B) In, airborne active surveillance, and air-to-air radar that can detect aircraft with or without transponders. Additional development, named Phase 2, for extending the MOPS to additional UAS categories and operations is underway.

One objective of the Phase 2 development seeks to define requirements for operations of UAS equipped with low size, weight, and power (SWaP) sensors, or low SWaP UAS. While ADS-B and active surveillance can fit in the payload of many medium-sized UAS, the large, high-power radar required by the Phase 1 MOPS is physically infeasible and/or economically impractical for many UAS operations. Low SWaP sensors have favorable payloads but provide smaller surveillance volumes. For safety and operational suitability, UAS pilots need sufficient alerting times to evaluate and execute DAA maneuvers in order to maintain separation defined by the DAA Well Clear (DWC). Thus, UAS equipped with Low SWaP sensors have speed restrictions to help ensure pilots have sufficient alerting time.

The UAS Integration in the National Airspace System (NAS) Project at NASA established partnership with Honeywell International in 2017 to conduct a shared resource project for further development of a prototype airborne low SWaP surveillance system. Honeywell provided a prototype airborne radar called DAPA-Lite as a candidate for validating and verifying proposed performance requirements for low SWaP surveillance systems within a DAA system. NASA provided UAS integration support as well as flight test planning and execution.

Flight Test 6 (FT6) was conducted at NASA Armstrong Flight Research Center from August to November 2019. The overall objective of FT6 was to collect data to inform the development of the Phase 2 DAA and low SWaP sensors’ requirements. FT6 was conducted in 3 configurations, each having its own sub-objective: Radar Characterization assessed the performance of Honeywell’s DAPA-Lite. Scripted Encounters validated the performance of a DAA system under a limited surveillance volume. Full Mission collected subject pilot’s performance data performing DAA tasks in a real-world test environment to validate previous human-in-the-loop simulations. This report focuses on analysis of the scripted encounters data.

The rest of the paper is organized as follows: Section 2 provides background information on DAA, and Section 3 describes flight operations. Section 4 discusses data analysis results, such as effectiveness of DAA maneuvers, flight card categorization, alerting performance, and trajectory errors.

2 Detect and Avoid

The DAA system aims to keep the UAS “well clear” of other manned aircraft. The DAA system consists of surveillance components, alerting and guidance algorithms, ground control station for UAS operator and pilot, and command and control systems. The DAA MOPS defines quantitatively a DWC around other aircraft the UAS should avoid. Alerts and guidance aim at assisting the UAS operator or pilot in maintaining separation defined by the DWC. The DAA MOPS also defines display requirements for alerts and guidance [7]. The DAA MOPS assumes the UAS is flying by instrument flight rules (IFR), and the UAS pilot or operator is expected to coordinate with air traffic control (ATC) for a conflict avoidance maneuver.

During the scripted encounters, a cylindrical DWC definition of 450 ft vertical separation and 2200 ft horizontal separation was utilized [8]. A loss of DWC (LoDWC) occurs when the horizontal and vertical separations are simultaneously violated [9].

The DAA alerting structure is comprised of three alert types: preventive, corrective, and warning. A preventive alert is a caution level alert that requires a maneuver to avoid a predicted DWC violation, but advises the pilot to maintain the UAS’s current altitude to avoid conflicts. A corrective alert is a caution level alert that advises the pilot to coordinate with ATC before maneuvering. A warning alert requires immediate action from the pilot to start maneuvering to maintain DWC [7]. The scripted encounters in FT6 only trigger corrective and warning alerts. Figure 1 shows the alerting timeline and the corresponding guidance.

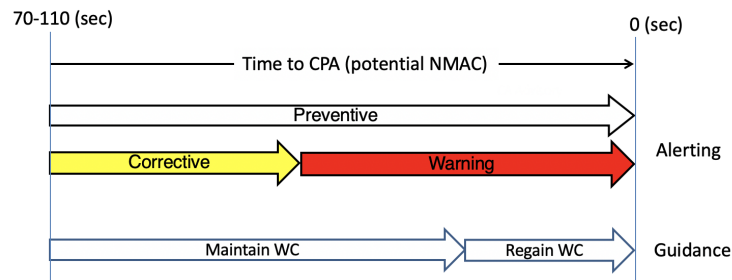


Figure 1: Alerting Timeline [7]

The guidance includes ranges of heading and altitude, shown as bands on a display system (see Section 3.6), predicted by the DAA system to have a high likelihood of leading to a LoDWC given a look-ahead time of typically 2 to 3 minutes. There is a

corresponding guidance type for each alert type. Aircraft performance parameters such as turn, climb, and descent rates can be used for computing the ranges of heading and altitude. To execute a DAA maneuver to maintain DWC, a UAS pilot is expected to select and maneuver the UAS to a heading or altitude that is outside the bands.

If the ownship gets too close to the intruder, a LoDWC may become inevitable even with maneuvers. In this situation, the guidance bands fill up all ranges of heading and altitude, but at the same time computes “regain well clear” bands to assist the ownship in maneuvering in order to regain well clear effectively. Regain-well-clear is also referred to as well clear recovery (WCR). For DAA systems assuming finite turn rates and climb/descent rates for the unmanned aircraft (UA), the WCR usually occurs earlier than a LoDWC during an encounter [7].

A DAA system’s surveillance components include ADS-B, active surveillance, and an onboard radar. ADS-B and active surveillance detect cooperative aircraft, i.e., aircraft that can broadcast ADS-B out messages and/or respond to interrogations by active surveillance. Both ADS-B and active surveillance have decent detection ranges beyond 10 nmi that provides more than enough alerting times for DAA. The onboard radar detects all aircraft, including the non-cooperative aircraft that are without a functioning transponder and cannot be detected by ADS-B or active surveillance. Previous research results show that, for low SWaP operations, a suitable surveillance range for the onboard radar lies between 2 and 3.5 nmi [7, 10], considering both safety and operational suitability metrics such as alerting timelines.

3 Flight Test Operations

FT6 was conducted at NASA Armstrong Flight Research Center, CA in restricted airspace R-2515. FT6 included radar characterization, scripted encounters, and full mission. Nine flight test days were dedicated to the scripted encounters from August 2019 to December 2019. The data analysis in this report focuses on the scripted encounters.

The following subsections are organized in this way: Section 3.1 presents the test aircraft. Section 3.2 discusses the encounter design. Section 3.3 describes the specific DAA algorithm for this flight test. Section 3.4 discusses the ground control station and its display. Section 3.5 describes the pilot procedure. Section 3.6 gives details of data collection and the post-processing steps.

3.1 Test Aircraft

The flight test elements consist of one ownship (the UA) and one intruder manned aircraft per encounter. A detailed introduction on the ownship and intruder is provided in this section.

The NASC TigerShark Block 3 XP (N1750X), equipped with the Honeywell DAPA-Lite radar for non-cooperative aircraft active surveillance, served as the ownship

during the scripted encounters. It is a medium-altitude and long-endurance single-engine pusher aircraft. The specifications of the Tigershark are shown in Table 1 [9].

Specification	Value
Wingspan	21.27 ft
Length	14.14 ft
Height	3.5 ft
Weight	515 lbs
Endurance	12 hr
Maximum Speed	80 KTAS
Stall Speed	47 KTAS

Table 1: Specifications of Tigershark [9, 11]

The T-34C Mentor (NASA865), TG-14 Super Ximango (NASA856), and Beechcraft B200 King Air (NASA801) served as the intruders. They were flown against the ownship to evaluate the performance characteristics of the Honeywell DAPA-Lite radar and the DAA system. The T-34C Mentor, TG-14 Super Ximango, and Beechcraft B200 King Air have a maximum speed of 214 kts, 132 kts, and 292 kts, respectively [9].

The TigerShark was equipped with ADS-B and Honeywell’s DAPA Lite radar. ADS-B detects manned aircraft that are equipped with ADS-B out. Three panels of DAPA-Lite Radar were installed at the nose of TigerShark and were expected to detect and track traffic within its theoretical field of regard ($\pm 15^\circ$ elevation and $\pm 110^\circ$ azimuth) regardless of whether that aircraft has other electronic means of identification [9].

The TigerShark’s Sagetech XP transponder offers ADS-B out capability, which provides position, altitude, velocity, and other information to the test team. The MXS transponder on the TigerShark receives NMEA GPS data from the Piccolo II autopilot through a serial interface. These data provided situational awareness of the Tigershark’s altitude and position to the test team during all of the FT6 flights. The intruder aircraft were also equipped with ADS-B out [9].

DAPA-Lite turned out to be unable to provide consistent tracks. Therefore, the test team decided to emulate a low SWaP sensor by filtering ADS-B surveillance data with a simulated surveillance volume. The simulated surveillance has a $\pm 15^\circ$ elevation range and $\pm 110^\circ$ azimuth range [9]. Its range (inter-aircraft distance) varies between 2.0, 2.5, and 3.5 nmi across encounters.

The UAS pilots controlled Tigershark through an auto-pilot system called Piccolo II. Piccolo II is a self-contained flight management computer that consists of built-in 3-axis accelerometers, 3-axis gyros, GPS, command and control radio, and various inputs/outputs to interface with external components (e.g. servos, research payloads, transponders). The pilots would type in a heading value in the Piccolo, then press “Send” to uplink the command. For FT6, Piccolo II provided NMEA GPS

messages to the Sagetech MXS ADS-B unit through a RS-232 serial interface. A second serial port on the autopilot was interfaced to the Unmanned Aircraft Processor (UAP) to provide telemetry from the air data system that was not available from the VN-210 EGI [9]. Towards the second half of the scripted encounters, pilots switched to Vigilant Spirit Control Station (VSCS) for issuing heading commands to be more representative of an integrated UAS where DAA information and vehicle commands would be executed from a common display.

3.2 Encounter Scenario Design

3.2.1 Encounter Geometry

There were several types of encounter geometries: Head-on, crossing, maneuvering intruder, ascending and descending intruder. The encounters included five different headings of the intruder relative to the ownship, 0° , 40° , 50° , 80° , 120° . At the closest point of approach (CPA), a combination of vertical and/or lateral offsets was required of each encounter for safety. The lateral offset was 0 nmi when the vertical offset was 500 ft, and 0.3 nmi when the vertical offset was less than 500 ft. The ascent rate and descent rate were either 500 fpm or 1000 fpm. For encounters with a maneuver intruder, the intruder turned into the ownship at a heading of 40° or 80° relative to the ownship.

DAA Encounter #	2.a.0.3	2.a.50.4	2.b.40.3	2.b.40.11	2.b.80.6	2.b.120.4	2.c.40.1	2.c.40.2	2.c.80.1	2.c.80.2	2.d.0.2	2.d.0.4
Angle Into Int 1	0	50	40	40	80	120	40	40	80	80	0	0
Vertical Offset Int 1 (ft)	200	200	200	200	500	200	500	500	500	500	1200	2200
CPA Lateral Offset INT1	0.3	0.3	0.3	0.3	0.0	0.3	0.0	0.0	0.0	0.0	0.0	0.3
GS OWN	60	60	60	60	60	60	60	60	60	60	60	60
GS INT1	170	170	100	170	100	170	100	100	100	100	100	100
Ownship Initial Altitude	8000	8000	8000	8000	8000	8000	8000	8000	8000	8000	8000	8000
Ownship Vertical Velocity	0	0	0	0	0	0	0	0	0	0	0	0
Ownship Final Altitude	8000	8000	8000	8000	8000	8000	8000	8000	8000	8000	8000	8000
Ownship Abort Alt	8000	8000	8000	8000	8000	8000	8000	8000	8000	8000	8000	8000
Intruder 1 Initial Altitude	7800	7800	7800	7800	7500	7800	7500	7500	7500	7500	6800	5800
Intruder 1 Vertical	0	0	0	0	0	0	0	0	0	0	500	1000
Intruder 1 Final Altitude	7800	7800	7800	7800	7500	7800	7500	7500	7500	7500	7800	7800
Intruder 1 Abort Alt	7000	7000	7000	7000	7000	7000	7000	7000	7000	7000	7000	7000
IP OWN	IP1	IP1	IP1	IP1	IP1	IP1	IP1	IP1	IP1	IP1	IP1	IP1
IP OWN Lat	34.8879	34.8879	34.8879	34.8879	34.8879	34.8879	34.8879	34.8879	34.8879	34.8879	34.8879	34.8879
IP OWN Lon	-117.6851	-117.6851	-117.6851	-117.6851	-117.6851	-117.6851	-117.6851	-117.6851	-117.6851	-117.6851	-117.6851	-117.6851
IP OWN DME	2	2	2	2	2	2	2	2	2	2	2	2
CPA OWN	CPA1	CPA1	CPA1	CPA1	CPA1	CPA1	CPA1	CPA1	CPA1	CPA1	CPA1	CPA1
CPA OWN Lat	34.8879	34.8879	34.8879	34.8879	34.8879	34.8879	34.8879	34.8879	34.8879	34.8879	34.8879	34.8879
CPA OWN Lon	-117.6445	-117.6445	-117.6445	-117.6445	-117.6445	-117.6445	-117.6445	-117.6445	-117.6445	-117.6445	-117.6445	-117.6445
IP INT1 Lat	34.8829	34.9652	34.9285	34.9535	34.9426	34.9740	34.8963	34.8963	34.9082	34.9082	34.8829	34.8829
IP INT1 Lon	-117.5293	-117.5708	-117.5937	-117.5574	-117.6327	-117.7048	-117.6075	-117.6075	-117.5984	-117.5984	-117.5768	-117.5768
IP INT1 DME	5.6667	5.6667	3.3333	5.6667	3.3333	5.6667	3.3000	3.3000	3.3000	3.3000	3.3333	3.3333
CPA INT1 Lat	34.8829	34.8929	34.8928	34.8928	34.8879	34.8922	34.8879	34.8879	34.8879	34.8879	34.8829	34.8829
CPA INT1 Lon	-117.6445	-117.6448	-117.6456	-117.6456	-117.6445	-117.6472	-117.6445	-117.6445	-117.6445	-117.6445	-117.6445	-117.6445
MP INT1							MP1	MP1	MP2	MP2		
MP INT1 LAT							34.8963	34.8963	34.9082	34.9082		
MP INT1 LON							-117.6324	-117.6324	-117.6401	-117.64		
MP INT1 DME							0.8	0.8	1.2	1.2		
Init Lateral dist (NM)							1.2	1.2	1.2	1.2		

Table 2: Scripted Encounters Flight Matrix

Table 2 lists ownship and intruder flight information. The flight matrix shows initial point (IP)'s & CPA's locations, angle of intruder's heading relative to the ownship, ownship's altitude & ground speed, intruder's altitude & ground speed, vertical offset, CPA lateral offset, climb or descent rate, and maneuver point's (MP) location for each encounter. The flight time between an IP and a CPA is 2 minutes.

A flight card for an encounter is comprised of 2 parts: ownship and intruder. Figure 2 and Figure 3 are dedicated to those ownship and intruder components, respectively. The flight card shows the top view graphics, horizontal view graphics, IP/CPA names and coordinates, altitudes, headings, distances, ground speeds, sensor selection, abort procedures, etc [9].

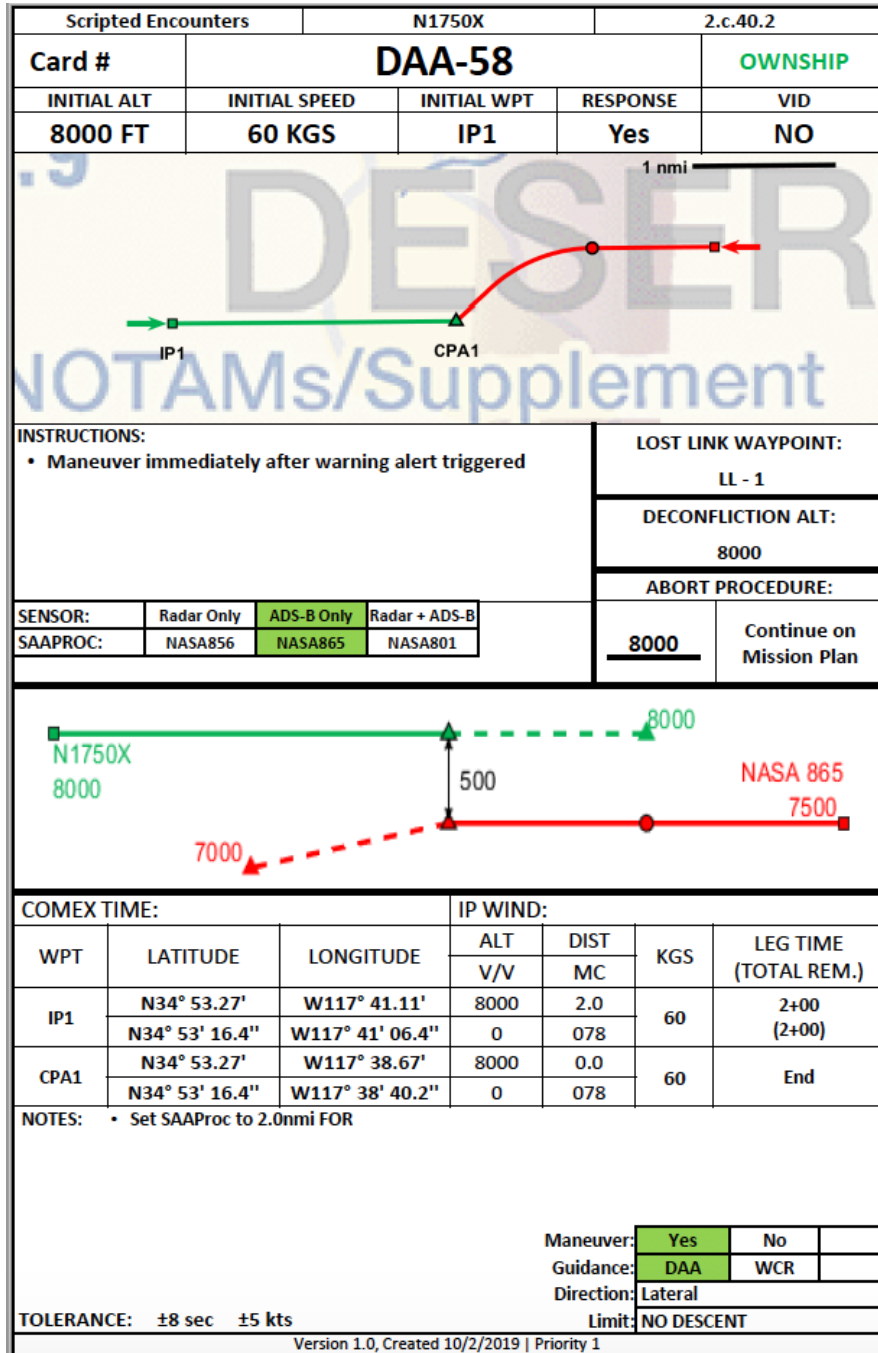


Figure 2: Flight card for the Ownship [9]

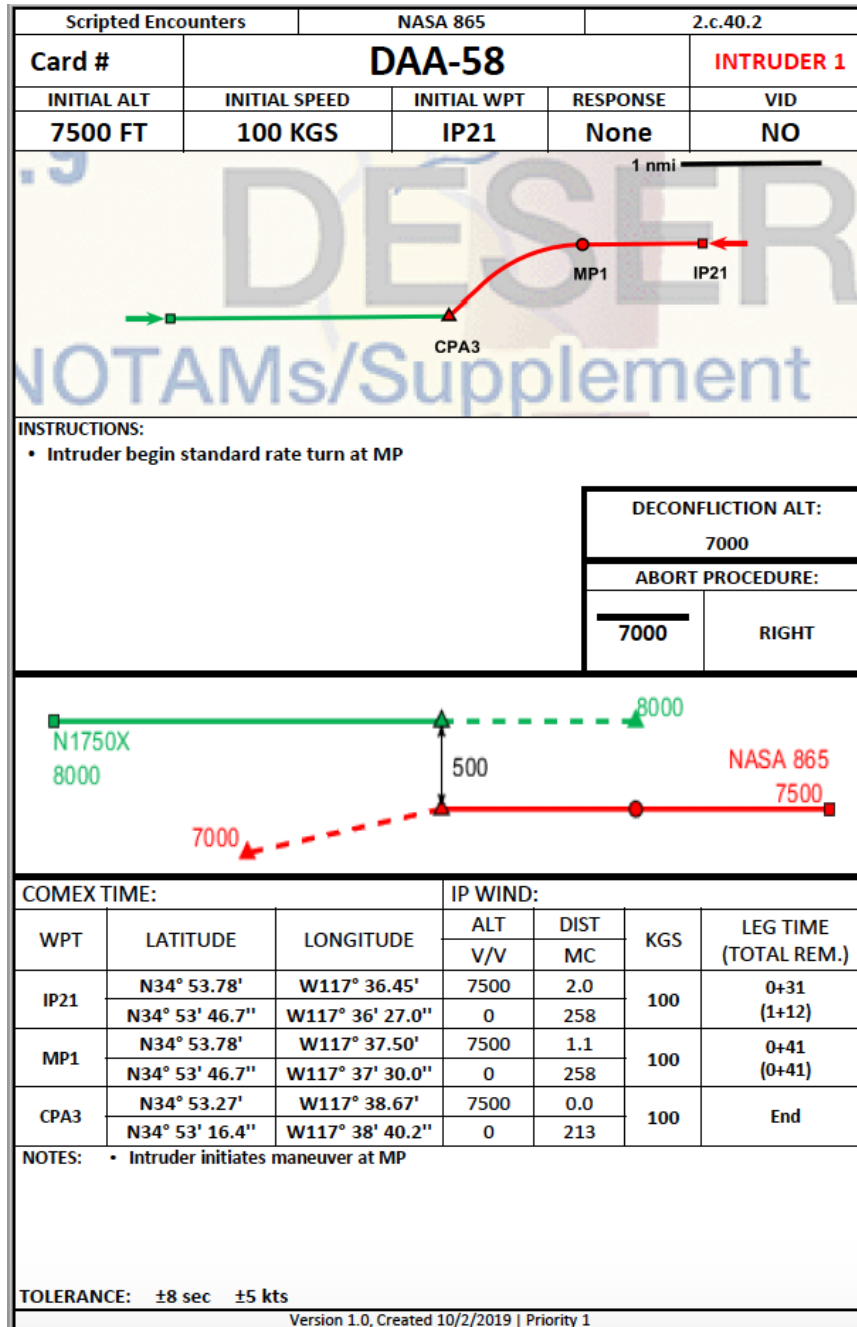


Figure 3: Flight card for the Intruder
[9]

Unmitigated encounters indicate that the ownship and intruder would maintain the predetermined flight path trajectories from the IP to the CPA. No aircraft makes maneuvers to avoid the imminent LoDWC. Conversely, mitigated encounters indicate that the UAS pilot was required to maneuver based on the maneuver guidance of the DAA system to avoid the imminent LoDWC. Data analysis in this report focuses on mitigated encounters.

3.3 Detect-and-Avoid Algorithm

The open-source Detect and Avoid Alerting Logic for Unmanned Systems (DAIDALUS) is a reference DAA algorithm for the Phase 1 MOPS [7]. The DAIDALUS reference implementation computations of alerts are based on alerters. An alerter consists of three sets of DWC thresholds labeled “FAR,” “MID,” and “NEAR.” The FAR, MID, and NEAR threshold values are intended to correspond respectively to the preventive, corrective, and warning alerting volumes and times. DAIDALUS’s guidance computation for this work is based on a constant turn rate, constant acceleration of the ownship, and constant-velocity projections of traffic aircraft. These bands are computed for the MID and NEAR threshold values provided in the alerter [6]. In DAIDALUS, a corrective alert was configured to indicate a predicted LoDWC within 60 seconds or less. A warning alert was configured to indicate a predicted LoDWC within 30 seconds or less. The vertical alerting threshold for both corrective and warning alerts was increased from 450 ft, the DWC’s vertical threshold, to a large value of 4000 ft. The purpose of expanding this threshold from 450 ft was to keep the alerts stable and remove the effect of vertical offsets in the flight cards on the alerts. The horizontal distance threshold was also increased from 2200 ft to 3342 ft in most encounters to reduce the impact of sensor uncertainties on the stability of alerts.

The maneuver guidance provided by DAIDALUS is presented in the form of conflict bands, i.e., ranges of headings and altitudes that lead to a well-clear violation, or recovery bands, i.e., ranges of ownship maneuvers that recover from a present or unavoidable well-clear violation. WCR will show up when the guidance band is saturated to maximize separation and avoid Near Mid-Air Collision (NMAC) [6].

During the flight test, DAIDALUS was invoked as a plug-in to the Java Architecture for DAA Extendibility and Model (JADEM) tool suite. JADEM saves aircraft states, alerts, and guidance data to files. An additional wrapper layer around JADEM, called SaaProc, provides real-time message handling, and filtering aircraft states by the intruder’s relative position to the ownship [9, 12].

3.4 Ground Control Station

The Research Ground Control Station (RGCS) consists of the VSCS with integrated JADEM & DAIDALUS DAA functionality, an interface to the Live Virtual Constructive (LVC) gateway, and a Plexsys voice communications link to the pseudo-pilot and ATC stations. DAA maneuvers were sent to Piccolo, which relayed them to the UA. Command and Control datalinks, comprised of an uplink and a downlink, to the UA were provided by a Piccolo-based Ground Control Station (GCS) and a Silvus Technologies radio system [9].

3.5 Pilot’s Background & Procedure

The recruited Subject Pilots Under Test (SPUTs) for FT6 were active military with a fixed wing license and have had recent flying experience including flying medium to large fixed wing remotely piloted aircraft within the last year [13].

During the scripted encounters, the UAS pilots were expected to select at their discretion a heading outside the conflict bands, i.e., a heading that was predicted to be conflict-free. WCR guidance was computed and displayed to pilots when the conflict bands saturate all the headings. In this situation, pilots were expected to select a heading within the range of the positive guidance provided by the WCR. The mitigated test matrix instructs the UAS pilot to execute a maneuver 8 seconds after a corrective alert is triggered or 3 seconds after a warning alert is triggered. Some flight cards required that the UAS pilot execute maneuver upon initiation of a warning alert or an alert that appears first. Results show that, due to various reasons, UAS pilots did not adhere strictly to the instructions regarding timing and, in some encounters, executed maneuvers very late.

3.6 Data Collection and Post-Processing

Data were collected during the flight test and post-processed. Figure 4 shows the data collection processes and post-processes. The solid arrows represent data flow in real time; the dotted arrows represent data flow in post-processing. The dashed boxes stand for processes or devices, and the solid boxes stand for data storage.

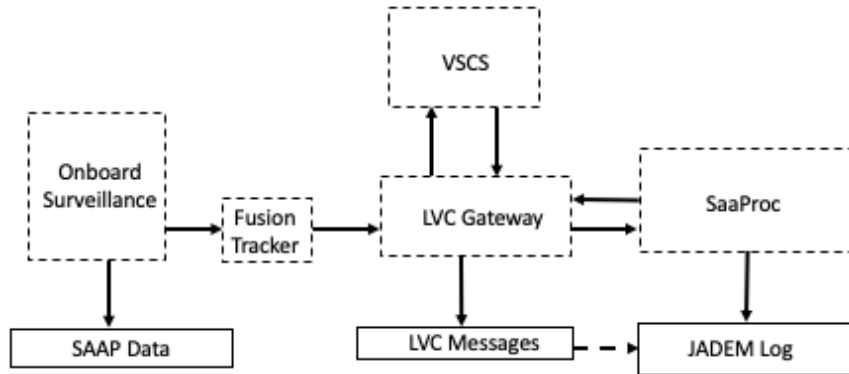


Figure 4: Data Flow Diagram

JADEM log files and LVC messages were two types of data collected and analyzed. They provided aircraft states, DAA alert and guidance, and pilots’ target maneuver course and heading data.

The Sense-and-Avoid Processor (SAAP) recorded and stored the ownship’s surveillance data from individual sensors. The surveillance data were sent to an onboard fusion tracker from Honeywell that performed track coordinate transformation, fil-

tering, association, and fusion. The LVC Gateway received flight state messages, time-stamped them, and forwarded them to the SaaProc [14]. The SaaProc read the flight states, computed alerts and guidance, and sent the guidance to the LVC Gateway. The LVC Gateway not only logged the flight state messages in LVC message files but also received guidance messages from SaaProc and forwarded them to VSCS. VSCS also sent pilot’s maneuvers to the LVC Gateway. SaaProc recorded the flight states, alerts, and maneuvers as JADEM log files [12].

It was necessary to post-process some flight test data to see if the alert was active when the pilot-selected avoidance maneuver heading was captured. FT6 LVC messages from the scripted encounters were post-processed into encounter files that included aircraft state using an LVC translator. Afterwards, the encounter files were utilized to re-compute alert and guidance using SaaProc configuration files that were configured to remove the simulated radar field of view to produce a new set of JADEM log files.

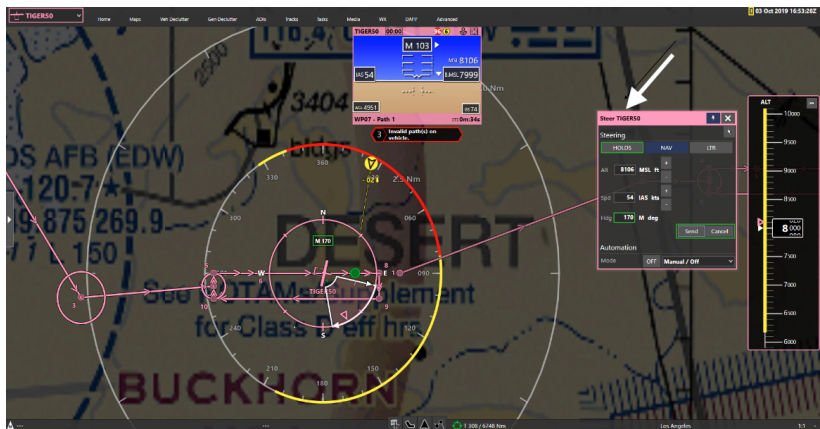


Figure 5: Vigilant Spirit Display

Figure 5 shows a corrective alert for the intruder. The color of the icon for the intruder indicates the threat level. The horizontal as well as the vertical guidance bands are shown on display. The white arrow points at the steering window where the UAS pilots use the Vehicle Steering Command, such as heading, altitude, and speed hold commands and Air Vehicle Position Waypoint command to control the UAS [9]. Only heading maneuvers were executed during the Scripted Encounters configuration.

4 Analysis and Results

4.1 Flight Cards Summary

System checkout (SCO) flights were flown in August of 2019 prior to the data collection days for radar characterization and scripted encounters (SE). Flight data from System Checkout flight days and scripted encounters showed good quality and

were included for data analysis. The flight days from which data are analyzed are SCO#5(08/13/19), SCO#6(08/22/19), SCO#7(08/28/19), SCO#8(08/29/19), SCO#9(09/24/19), SE1(10/01/19), SE2(10/03/2019), SE3(10/08/2019), and SCO#10(10/16/19). A total of 96 encounters were attempted. Among these 96 encounters, 72 led to a collection of alerting and guidance data successfully. The other 24 encounter data was not collected due to the triggering of improper alerts. The total flight hours were 29.8.

4.2 Categorization by Maneuver Outcomes

4.2.1 Flight Card Categorization Scheme & Statistics

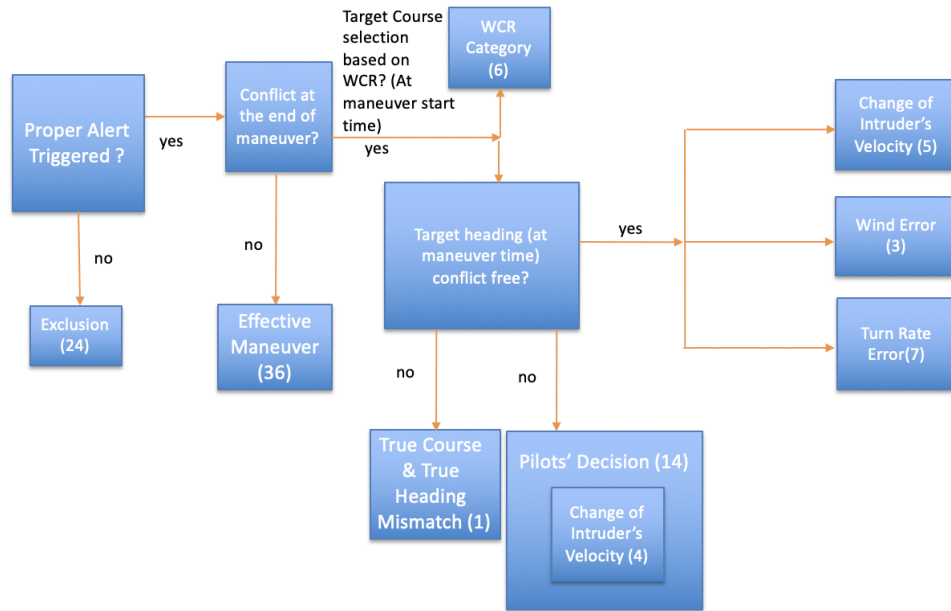


Figure 6: Categorization by Maneuver Outcomes (Number of Encounters in Associated Classification)

Figure 6 depicts the overall maneuver outcome categorization. Data analysis focused on the 90 mitigated encounters. These encounters were classified based on the outcome of alert, guidance, and effectiveness of pilots' maneuver in resolving conflicts. Twenty-four encounters were excluded from additional analysis due to data issues such as segmentation fault on the UAP computer. The remaining encounters were 66.

A maneuver was ineffective if, at the completion of the maneuver, the alert was still active. Among the 66 encounters analyzed for maneuver effectiveness, 36 of these had maneuvers effectively resolving conflicts. Six encounters with maneuvers based on WCR were also excluded. The remaining encounters with ineffective maneuvers were further analyzed for potential causes. Among those 30 encounters with ineffective maneuvers, fourteen were attributed to pilots' decisions, one attributed to

a true heading/true course mismatch, and the other 9 were attributed to trajectory prediction errors. Three sources of trajectory prediction errors were analyzed: change of intruder’s velocity, wind error, and turn rate error. An encounter could exhibit multiple sources of trajectory error. Six of the encounters in the pilots’ decision category also had contributions from change of intruders’ velocities. The lead contributing factors were pilots’ decision and change of intruders’ velocities.

During the scripted encounters flight test phase, a true heading and true course mismatch issue in the maneuver guidance execution was found. Pilots selected a horizontal maneuver based on the true heading conflict bands shown on the DAA display. However, when the maneuver was inputted to Piccolo, its heading value was interpreted by Piccolo as a true course. This mismatch caused the actual maneuver to deviate slightly from the intended one, the degree of which varies with the wind condition. It is necessary to investigate whether the corresponding target heading is in the conflict band at the maneuver. Target heading θ_h & target course θ_c difference is given by

$$|\theta_h - \theta_c| = \arccos\left(\frac{V_{tas}^2 + V_g^2 - V_w^2}{2V_{tas}V_g}\right) \quad (1)$$

Target heading θ_h is given by

$$\theta_h = \theta_c + \arccos\left(\frac{V_{tas}^2 + V_g^2 - V_w^2}{2V_{tas}V_g}\right) \quad (2)$$

or

$$\theta_h = \theta_c - \arccos\left(\frac{V_{tas}^2 + V_g^2 - V_w^2}{2V_{tas}V_g}\right) \quad (3)$$

Target heading θ_h can be calculated using Eq. 2 or Eq. 3 depending on the trigonometric relationship between the wind speed vector \vec{V}_w , true airspeed vector \vec{V}_{tas} , and ground speed vector \vec{V}_g .





Target Course Target Heading		
	Pilots' Decision	True Course & True Heading Mismatch
	Mismatch but Good Decision	Good Decision

Figure 7: Target Course & Target Heading Decision Chart

Figure 7 shows whether the target heading or/and target course is/are conflict-free at the time of maneuver. The time of a maneuver is estimated from the ownship’s state data by observing the first time the ownship started turning. Note this time may be a few seconds after the time the pilot submitted the heading command on the ground due to the system’s latency. The circle represents “conflict-free,” and the

cross represents “in conflict.” When both the target heading and the target course are in the conflict band, it will be called “Pilots’ Decision.” If the target heading is in conflict, but the target course is conflict-free, it will be called “True Course & True Heading Mismatch.” The sources of error, such as change of intruder’s velocity, wind error, and turn rate error, will be analyzed when the target heading is conflict-free.

4.2.2 Explanations of Categories with Examples

I. Exclusion

The exclusion category indicated that alerts were not properly triggered, or there were technical difficulties getting the data. When the timing was off, alerts were unstable, or Sensor Uncertainty Mitigation (SUM) led to very early WCRs, the flight cards were considered having improper alerts. The encounters were excluded if the segmentation faults occurred on the UAP computer that managed the payload, or data were not obtained.

II. Maneuver upon Well Clear Recovery

The pilots selected a target heading based on the WCR guidance at the maneuver. Maneuvering upon WCR was undesirable because the UAS pilots maneuvered late. Figure 8 shows an example of WCR. The upper left panel shows the true course and true heading of the ownship v.s. time. The red color and green color indicate the warning band and the WCR guidance, respectively. The upper mid panel shows the trajectories for the ownship and the intruder. The upper right panel shows the distance between the ownship and the intruder as the time elapses. The bottom left panel shows the wind direction relative to the true north measured from the ownship. The bottom middle panel shows the ground speed for the ownship and the intruder as well as the wind speed. The bottom right panel shows ownship’s turn rate as the time elapses.

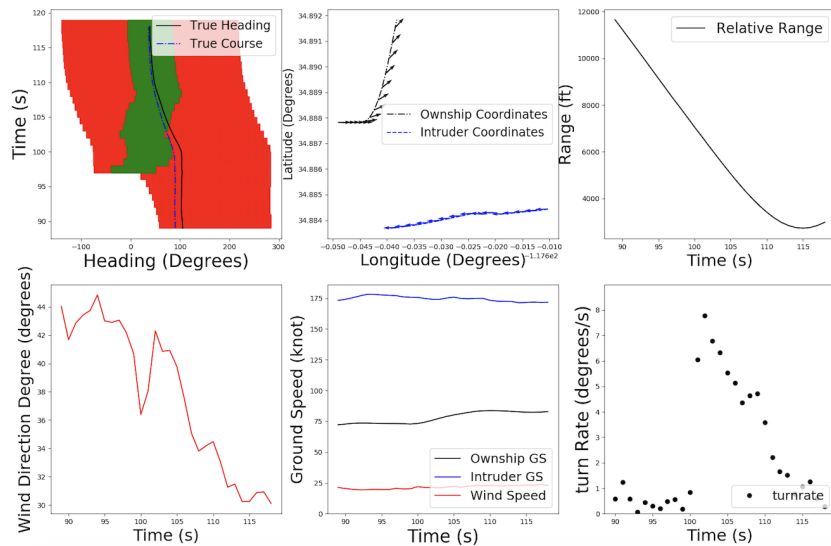


Figure 8: Example of WCR

III. Effective Maneuver

Effective maneuver indicated that the ownship was conflict-free at the end of the maneuver. Namely, all the alerts disappeared when the turn was completed. There were 34 effective maneuvers. Figure 9 presented an example of an effective maneuver.

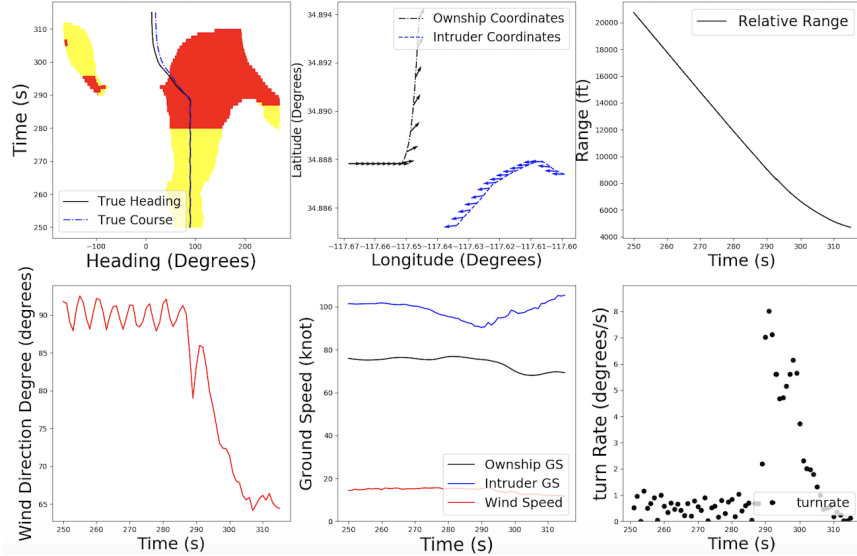


Figure 9: Example of an Effective Maneuver

IV. Pilots' Decision

Pilots' decision indicated that the ineffectiveness of the maneuvers was caused by both the target course that the pilots selected and its calculated target heading in the conflict bands. Figure 10 presented an example of pilots' decision.

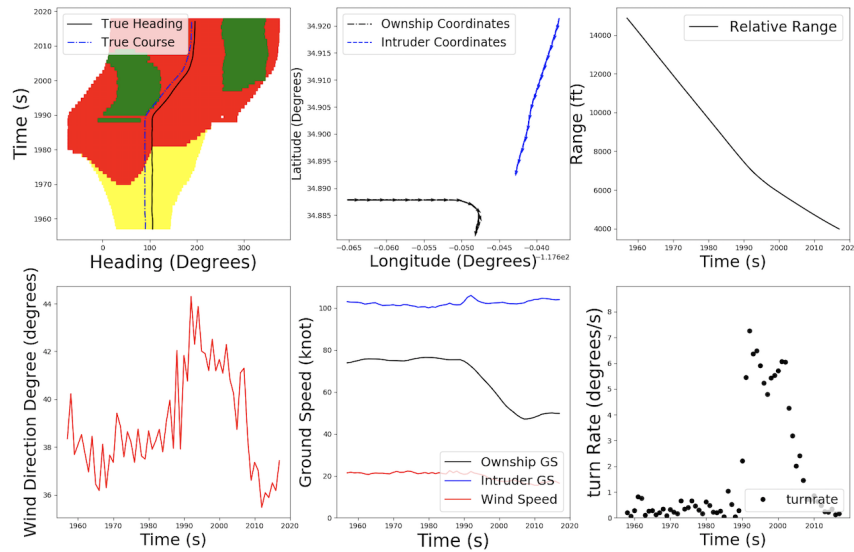


Figure 10: Example of Pilots' Decision

V. True Course & True Heading Mismatch

The target course was outside the conflict band; however, its calculated target heading was inside the conflict band. Figure 11 presented an example of true course & true heading mismatch.

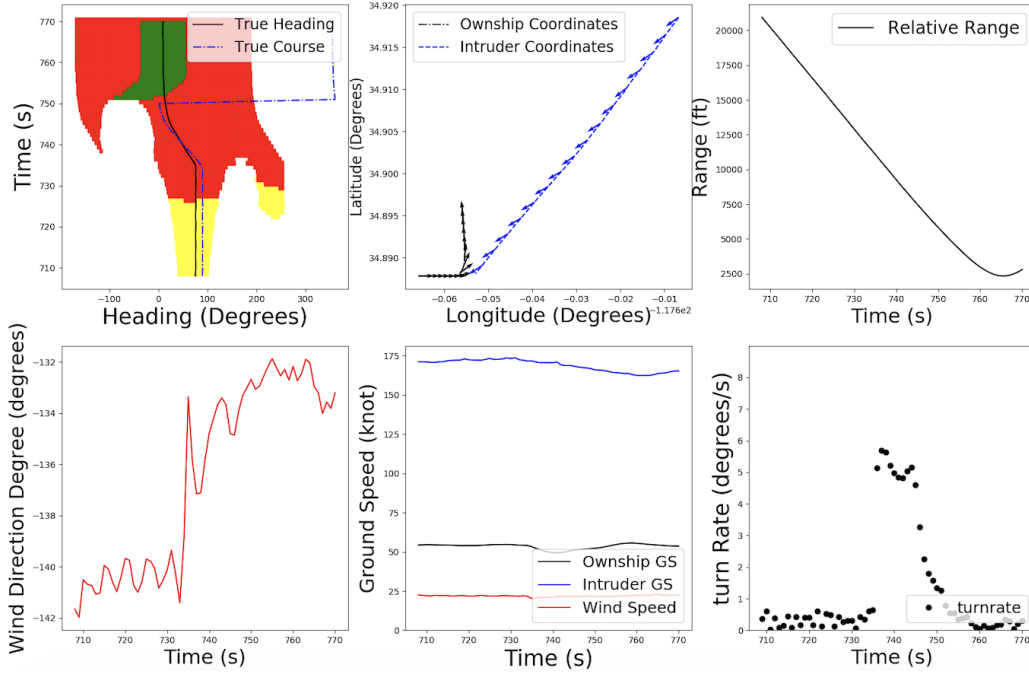


Figure 11: Example of True Course & True Heading Mismatch

VI. Change of Intruder's Velocity

The criteria is given by

$$|\Delta \vec{V}_{int}| = |\vec{V}(t)_{int} - \vec{V}_{start, M, OS}| \geq 10kts \quad (4)$$

According to Eq. 4, the change of intruder's velocity is calculated by the magnitude of the vector difference between the intruder's velocity as a function of time and intruder's velocity at the start of ownship maneuver. There were five encounters in this category. Three out of the total five encounters had a maneuvering intruder. Figure 12 shows an intruder that kept turning, which caused difficulty to the DAA algorithm. A right turn appeared to be feasible for resolving the conflict at one time. However, the intruder maneuver "closed the gate" afterwards. According for intruder's accelerations may improve predictions.

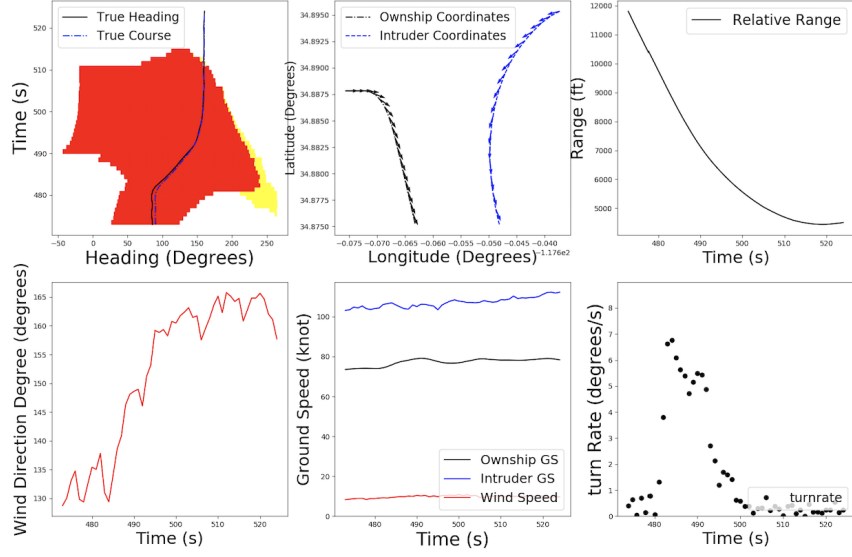


Figure 12: Example of Change of Intruder's Velocity

VII. Wind Error

The criteria is given by

$$\frac{|\vec{w}_f - \vec{w}_i|}{|\vec{w}_i|} \geq 40\% \quad (5)$$

If the magnitude of the vector difference between the wind velocity before the maneuver \vec{w}_i and wind velocity after the turn is completed \vec{w}_f is over 40% of the magnitude of wind velocity $|\vec{w}_i|$ before the maneuver, the encounter will be classified as wind error. There were three encounters that belonged to this category. Figure 13 shows an encounter where both the magnitude of the wind velocity and the wind direction change were large.

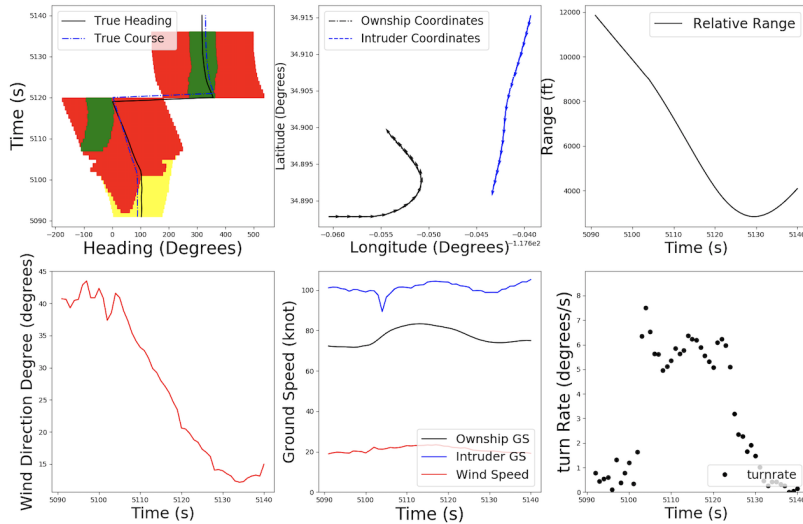


Figure 13: Example of Wind Error

VIII. Turn Rate Error

The criteria is given by

$$\frac{|\Delta t_{act} - \Delta t_{pred}|}{\Delta t_{pred}} \geq 50\% \quad (6)$$

If the difference between the actual turn time Δt_{act} and the predicted turn time Δt_{pred} is over 50% of Δt_{pred} , the encounter will be considered having turn rate error. Δt_{pred} is calculated using a standard turn rate of 7 deg/s, and Δt_{act} is measured from the start of the turn to the end of the turn with a cutoff turn rate of 0.75 deg/s. When the turn is small, the turn error tends to be larger because of its lower average turn rate. There were seven encounters in turn rate error category. Figure 14 presents an encounter where the turn rate error was 87.36 % and had an average turn rate of 3.48 deg/s because of its small turn.

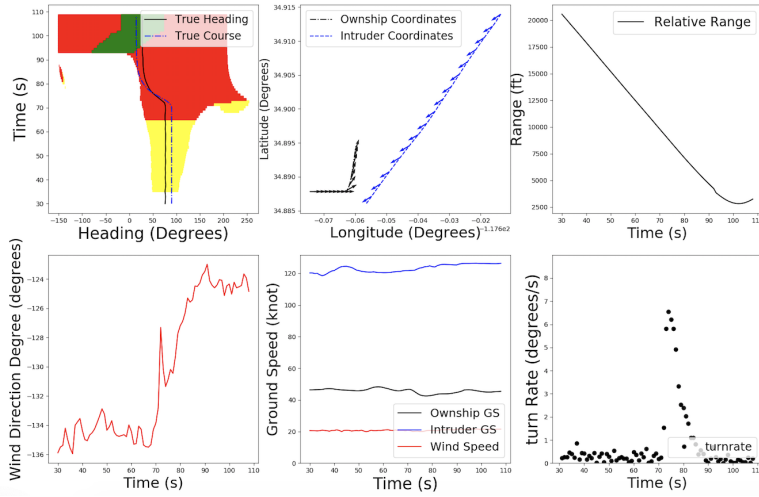


Figure 14: Example of Turn Rate Error

4.3 Breakdown by Surveillance Range

For the mitigated encounters, a simulated surveillance range was chosen to be 3.5 nmi, 2.5 nmi, and 2.0 nmi, which were potential candidates for required surveillance ranges for low SWaP sensors. The number of encounters that were flown with 3.5 nmi, 2.5 nmi, and 2.0 nmi surveillance ranges is 35, 36, and 19, respectively. After removing the flight cards from the exclusion and WCR category, the effectiveness and ineffectiveness rates for each surveillance range were tabulated in Table 3. Results suggest that encounters with 3.5 nmi had a higher probability of achieving effective DAA maneuvers.

Surveillance Range	Effectiveness	Ineffectiveness
2.0 nmi	54 %	46 %
2.5 nmi	55 %	45 %
3.5 nmi	72 %	28 %

Table 3: Effectiveness & Ineffectiveness Breakdown by Surveillance Range

4.4 Trajectory Error Analysis

The DAIDALUS modeled the turn using an infinite roll rate at the start of the maneuver and at the end of the turn and a fixed turn rate during the turn. A simulation was run to emulate the turn using the initial and target conditions from the ownship state data collected during FT6. Initial conditions for the trajectory error simulation were wind speed, wind direction, true course, altitude, aircraft position, and aircraft ground speed with a standard turn rate of 7 deg/s. Target conditions were altitude, true course, and true heading. Wind speed, wind direction, aircraft ground speed, and altitude were held constant in the simulation.

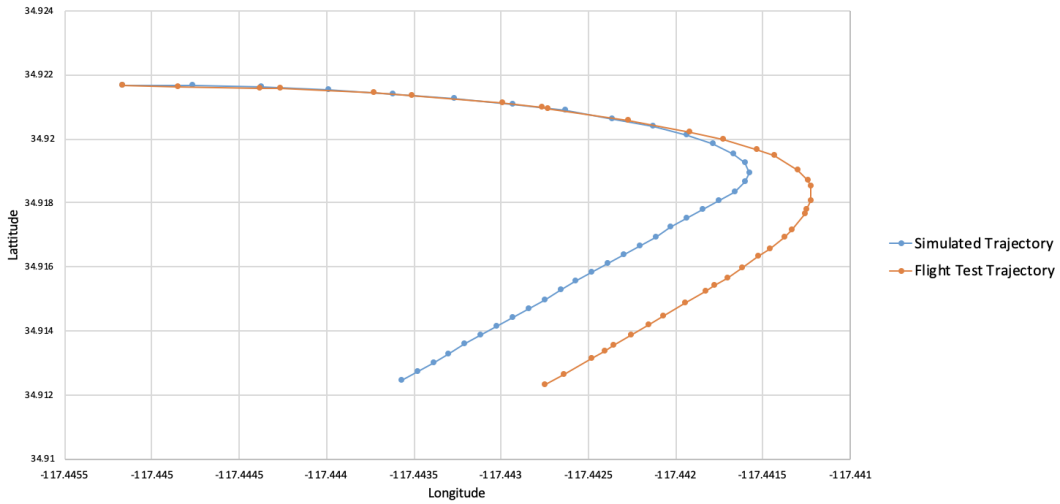


Figure 15: Trajectory Comparison

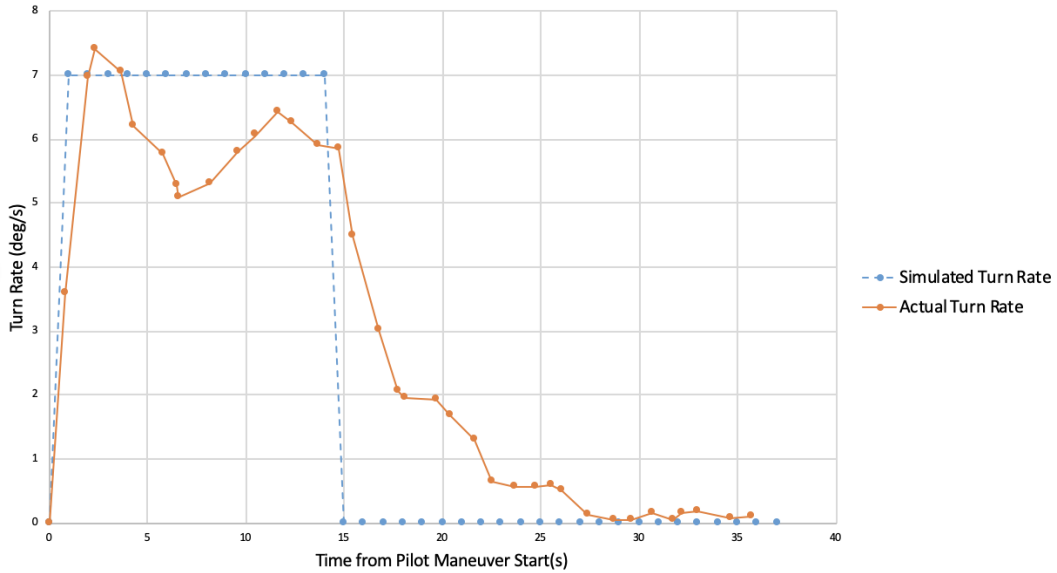


Figure 16: Simulated Turn Rate & Actual Turn Rate

Figure 15 shows the discrepancy between the simulated and actual trajectories during the turn and after the turn. The simulated trajectory turned faster compared to the actual flight test trajectory. Figure 16 shows that the turn rate for the simulated turn was at 7 deg/s during the turn; however, the actual turn rate was increased to 7.4 deg/s within the first few seconds, then fluctuated between 5 to 7 deg/s, and eventually went down.

Figure 17 indicates that the majority of the maximum turn rates for mitigated encounters was between 6 to 8 deg/s. The FT6 data showed that the range of turn rate was reasonable.

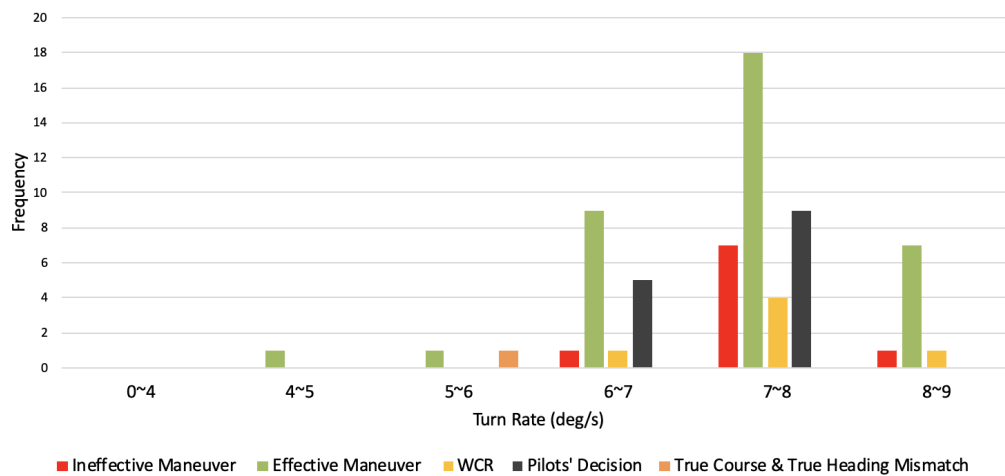


Figure 17: Turn Rate Histogram

4.5 Buffered Heading and Encounter Effectiveness Analysis

Adding a buffer to the DAA’s suggested minimum turn angle creates a “buffered heading.” Figure 18 depicts how the buffered heading affected the effectiveness of the encounters. The analysis likely included the effects of the mismatch between true course and true heading, but the effect on the overall results is expected to be minor. The angle was calculated using the difference between the target course & the edge of the conflict band. When the angle was negative, the target course was in conflict. If the angle was positive, the target course was conflict-free. If the angle was less than -75 deg, band saturation might have occurred. The majority of the ineffective encounters had pilots’ maneuvers inside the conflict band. Whereas, maneuvers were more effective when buffers were larger. Therefore, adding more buffer to the target heading may increase the probability of effectiveness.

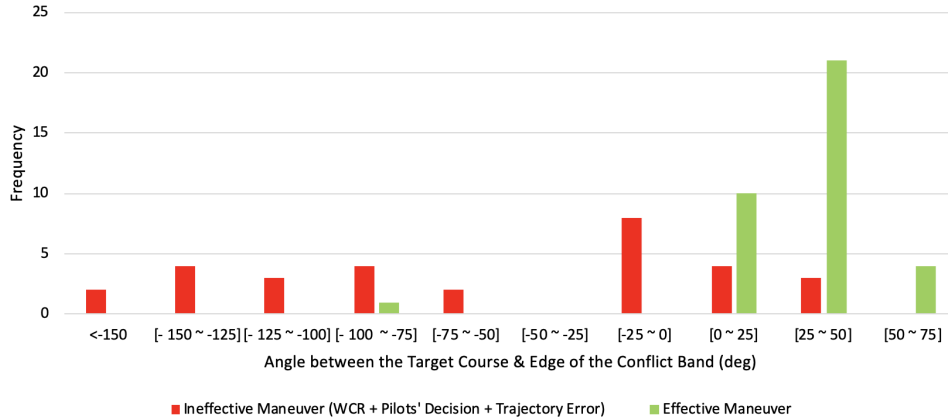


Figure 18: Buffered Heading & Encounter Effectiveness Histogram

5 Conclusions

The analysis of FT6 data was focused on classifying mitigated encounters based on the effectiveness of the DAA maneuver in resolving conflicts. For maneuvers executed in a timely fashion before WCR, more than half of these maneuvers effectively resolved conflicts. When categorized by surveillance range, a 3.5 nmi surveillance range achieved a higher success rate (about 70%) than 2.5 and 2.0 nmi (about 50%). Enlarging the surveillance range from 2.0 nmi and 2.5 nmi to 3.5 nmi increased the effectiveness of the maneuver.

When the maneuver turned out to be ineffective, additional analysis was done to determine the cause(s) of the ineffectiveness, such as pilots' decision, the true course and true heading mismatch, and trajectory prediction errors. Three main sources of trajectory prediction error were analyzed: change of intruder velocity, wind error, and turn rate error. Among all the ineffective encounters, the major contributing causes are pilots' decision and change of intruders' velocities.

When analyzing the category of change of intruder's velocity, it was observed that maneuvering intruders presented a challenging case for the DAA algorithm. The data show that accounting for potential accelerations in the intruder's trajectory should be strongly considered for future flight tests.

Trajectory error analysis successfully showed the discrepancies between the actual and simulated turn rates. Besides, the actual and simulated trajectories were plotted graphically to show the deviation between the two.

Buffered heading & encounter effectiveness analysis was conducted. It was ascertained from the results that it may be beneficial for pilots to add more buffer to the target heading to increase the maneuver effectiveness.

References

1. Wu, M. G.; Cone, A. C.; Lee, S.; Chen, C.; Edwards, E. W. M.; and Jack, D. P.: Well Clear Trade Study for Unmanned Aircraft System Detect And Avoid with Non-Cooperative Aircraft. *18th AIAA Aviation Technology, Integration, and Operations Conference*, AIAA-2018-2876, June 2018. URL <https://arc.aiaa.org/doi/pdf/10.2514/6.2018-2876>.
2. Vincent, M. J.; Trujillo, A.; Jack, D. P.; Hoffer, K. D.; and Tsakpinis, D.: A Recommended DAA Well-Clear Definition for the Terminal Environment. *2018 Aviation Technology, Integration, and Operations Conference*, AIAA-2018-2873, 2018. URL <https://doi.org/10.2514/6.2018-2873>.
3. Cook, S. P.; Brooks, D.; Cole, R.; Hackenberg, D.; and Raska, V.: Defining Well Clear for Unmanned Aircraft Systems. *Proceedings of AIAA Infotech@ Aerospace*, AIAA-2015-0481, AIAA, 2015. URL <https://doi.org/10.2514/6.2015-0481>.
4. Johnson, M.; Mueller, E. R.; and Santiago, C.: Characteristics of a Well Clear Definition and Alerting Criteria for Encounters between UAS and Manned Aircraft in Class E Airspace. *Eleventh UAS/Europe Air Traffic Management Research and Development Seminar*, 2015, pp. 23–26. URL <https://ntrs.nasa.gov/search.jsp?R=20190027490>.
5. *Minimum Operational Performance Standards (MOPS) for Detect and Avoid (DAA) Systems*. DO-365, RTCA. Inc., 2017.
6. *Minimum Operational Performance Standards (MOPS) for Air-to-Air Radar for Traffic Surveillance*. DO-366, RTCA. Inc., 2017.
7. Wu, M. G.; Cone, A. C.; and Lee, S.: Detect and Avoid Alerting Performance with Limited Surveillance Volume for Non-Cooperative Aircraft. 2019. URL <https://doi.org/10.2514/6.2019-2073.c1>.
8. Cone, A. C.; Wu, M. G.; and Lee, S.: Detect-and-Avoid Alerting Performance for High-Speed UAS and Non-Cooperative Aircraft. Jun 2019. URL <https://arc.aiaa.org/doi/pdf/10.2514/6.2019-3313>.
9. Vincent, M.; Wu, G.; Rorie, C.; Kim, S.; Marston, M.; Flock, A.; Hoang, T.; and Navarro, R.: Integrated Test and Evaluation (IT&E) Flight Test Series 6 Flight Test Report.
10. Chen, C. C.; Gill, B.; Edwards, M. W. M.; Smearcheck, S.; Adami, T.; Calhoun, S.; Wu, M. G.; Cone, A. C.; and Lee, S.: Defining Well Clear Separation for Unmanned Aircraft Systems Operating with Non-cooperative Aircraft. AIAA, 2019. URL <https://arc.aiaa.org/doi/pdf/10.2514/6.2019-3512>.
11. Marston, M.; Kim, S.; Loera, V.; Vincent, M.; and Navarro, R.: Integrated Test and Evaluation (IT&E) Flight Test Series 6 Flight Test Plan Document.

12. Gong, C.; Wu, M. G.; and Santiago, C.: UAS Integration in the NAS Project: Flight Test 3 Data Analysis of JADEM-Autoresolver Detect and Avoid System. , Dec 2016.
13. Bridges, W.; and Zach, R.: UAS-NAS Flight Test Series 6, Ames Research Center Test Report, 2020.
14. Soler, G.; Jovic, S.; and Murphy, J.: RUMS-Realtime Visualization and Evaluation of Live, Virtual, Constructive Simulation Data. AIAA, 2015. URL <https://ntrs.nasa.gov/search.jsp?R=20160007498>.